
ELSEVIER

Nuclear Instruments and Methods in Physics Research B 146 (1998) 190–197

NIM B
Beam Interactions with Materials & Atoms

Luminescence in thin molecular samples by bombardment with single MeV atomic ions

K. Koch [a], W. Tuszynski [a,*], Ch. Tomaschko [b], H. Voit [b]

[a] *Carl von Ossietzky-Universität, Fachbereich Physik, D-26111 Oldenburg, Germany*
[b] *Universität Erlangen-Nürnberg, Physikalisches Institut, D-91058 Erlangen, Germany*

Abstract

The luminescence induced by the bombardment of thin molecular samples with single MeV atomic ions has been measured by time-correlated single photon counting. The MeV-energy ions ($Z = 6...79$) were produced at the Erlangen tandem accelerator. The samples were layers of POPOP or CsI deposited on a thin polyester foil at a thickness which allows the ions to traverse the samples. The relative photon yield has been found to be proportional to the energy density along the ion trajectory when the initial velocity is kept constant. When the initial velocity of the primary ion was varied, a distinct maximum of the photon yield has been found which is clearly shifted to higher energies compared to the energy of the Bragg maximum. By means of calculations based on the energy deposition of the secondary electrons it was found that the observed luminescence is only produced in the region of low energy density at larger radial distances from the ion track.

PACS: 78.70.-g
Keywords: Swift heavy ion; Luminescence; Secondary electron energy density; Thin layer

1. Introduction

The luminescence produced in solid samples by the impact of high energy ions was recently the subject of several investigations in which the technique of time-correlated single photon counting has been applied for achieving highest detection sensitivity [1–4]. The experiments were made with ^{252}Cf-fission fragments having MeV-energies and with ions in the keV-energy range. The results obtained show that the photons produced by impinging high-energy ions (i) are prompt, (ii) are not correlated with a desorption of particular secondary ions, and (iii) come from radiative transitions within the bulk of the sample due to relaxations of the electronic system. The observed photon spectra gave evidence that the photons originate from the fluorescence of intact molecules or from the decay of self-trapped excitons. Indications that the excitation of molecules by secondary electrons is the necessary step in the fast heavy ion-induced luminescence process were also found experimentally.

* Corresponding author. Tel.: +49 441 798 3203; fax: +49 441 798 3201; e-mail: tuszynski@cip.physik.uni-oldenburg.de

0168-583X/98/$ – see front matter
PII: S0168-583X(98)00451-0

In the past, much experimental and theoretical work on the luminescence induced by high-energy ions was made. The aim of these papers was mainly to measure and to describe the luminescence response of scintillator detectors (see for example [5–7]). First experimental studies of *thin* films of fluorescent materials (μm-range) excited by individual *transiting* MeV-energy ions ($Z = 1...53$) were done in 1974 by Muga et al. [8,9]. The authors formulated a new model in which the *number* of electrons scattered perpendicular to the ion trajectory is taken as proportional to the luminescence response. They introduced also the concept of saturation of luminescence by supposing that above a critical electron number density all luminescence centers are excited and no additional response is generated. The calculated specific luminescence values were in good agreement with their experimental data.

In a recent theoretical publication, a model of ion-induced luminescence based on the *energy deposition* by secondary electrons has been proposed [10]. In this model, it is assumed that the local density of energy carriers, i.e. of electron-hole pairs or excited molecular structures, is proportional to the energy deposition. In the quenching region, the energy carrier density reaches a constant maximum value. The luminescence was taken proportional to the deexcitation of the energy carrier density. The fundamental variables of the incident ion characterizing the luminescence were found to be the *velocity* and the *effective charge*. The corresponding variables of the sample are average charge and mass of the sample compound, mass density and the energy density at which the quenching of the energy carrier density starts. The model was compared with experimental data with good results.

In this paper, new experimental results on the luminescence induced in thin molecular samples by the impact of single atomic MeV-energy ions are presented. The luminescence has been measured by *time-correlated single photon counting*. The MeV-energy ions ($Z = 6...79$) were produced at the Erlangen tandem accelerator allowing the ion parameters to be varied within a wide range. The samples were thin layers of POPOP or CsI. Their thickness was in the range of a few μm so that the ions could *traverse* the samples. The experimental results are explained qualitatively by calculated data obtained by applying the formalism of [10].

2. Experimental

2.1. Production of atomic MeV-ions

Various atomic MeV-energy ion beams produced at the Erlangen tandem accelerator were applied. The value of the ion flux was about 1000 s^{-1} and the typical ion fluence for accumulating one time profile was 10^8 cm^{-2}. The relative photon yields did not show any dependence on the flux as well as on the fluence in this range of values. A ^{127}I beam at 42 MeV was used for probing the effect of sample thickness. For bombarding with various primary ions of the same velocity, the ion beams listed in Table 1 have been generated. The corre-

Table 1
Primary ions used to measure the photon yield from a 1 μm POPOP and a 1.5 μm CsI sample. The ions had roughly the same initial velocity $v \approx 7.5 \times 10^6$ ms^{-1}. The mean electronic stopping power $(dE/dx)_e$ for the POPOP sample (TRIM calculation) is given in column 3. The effective charge of the ions z^* was calculated according to Eq. (2).

Primary ion	Energy/MeV	$(dE/dx)_e$/[MeV/μm]	z^*
^{12}C	4.0	1.13	3.87
^{16}O	5.3	1.50	4.55
^{32}S	10.6	3.13	6.40
^{63}Cu	20.6	4.88	8.26
^{108}Ag	35.8	6.63	9.99
^{127}I	42.1	6.75	10.46
^{197}Au	65.3	9.00	12.13

sponding values of the mean electronic stopping power $(dE/dx)_e$ calculated by the TRIM code [11] for bombarding a POPOP sample, and the values of the effective charge according to Eq. (2) are also listed in Table 1. When bombarding with ions of various velocities, a ^{32}S beam at energies as listed in Table 2 was used. The velocity of all ions used exceeds three times the Bohr velocity. This means that the energy loss in matter of these ions can be described by means of the Bohr–Bethe–Bloch formalism using appropiate values for the effective charge of the ions [12].

2.2. Setup

The experimental setup for measuring the luminescence emitted under the bombardment of single atomic MeV-energy ions is depicted in Fig. 1. The photons were produced in a vacuum recipient in which the accelerated ions were led after passing two 90° magnets. After passing also a last aperture, the ions impinged on the target. A silicon detector mounted behind the target registered the transmitted ions. The Si-detector signal was amplified, analyzed by pulse height to determine the ion energy and formed by a constant fraction discriminator (Ortec Quad CFD 934). The CFD output pulses were used to start a time-to-digital converter (CTN/M2, IPN, Orsay, France). To collect the photons produced in the sample, an optical fiber (diameter: 1 mm, black coated) was inserted into the recipient. The front face of the optical fiber was directed to the center of the target

Table 2
Initial energies E_0 of the applied ^{32}S primary ions and their average velocities $\langle v \rangle$ when traversing a 0.65 μm POPOP sample deposited onto a 2.1 μm polyester foil.

E_0/[MeV]	$\langle v \rangle$/[10^6 m/s]
14	7.47
20	9.44
28	11.76
32	12.77
36	13.71
45	15.60
50	16.57
55	17.45
60	18.31

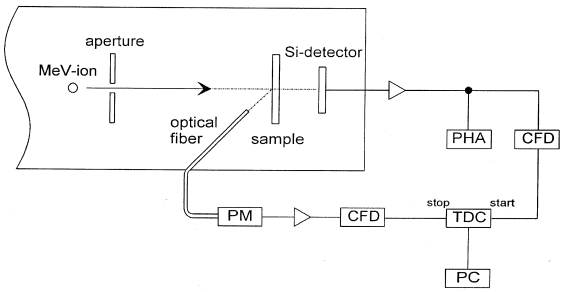

Fig. 1. Experimental setup for time-correlated counting of single photons produced by the impact of MeV-ions; PM: photomultiplier, CFD: constant fraction discriminator, TDC: time-to-digital converter, PHA: pulse height analyzer, PC: personal computer.

at a distance of about 5 mm and under an angle of about 20° to the surface normal of the target (the fiber was protected against strikes of incident ions). The other end of the fiber was mounted at the entrance window of a photomultiplier tube (Hamamatsu R269) that was placed outside the recipient. The photodetector was kept at −20°C to reduce the thermal background (to about 30 counts/s). The accessible spectral range is 300–750 nm (corresponding to 1.7...4.1 eV) limited by transmission of the optical fiber and by detector response. The samples are nearly transparent with regard to the produced luminescence. The luminescence of the laser dye POPOP is molecular fluorescence ranging from about 400 to 550 nm in our solid samples. The fluorescence maximum is at about 450 nm [2]. The luminescence of CsI originates from the decay of self-trapped excitons as described for example by [13]. There are two bands with maxima at 288 nm and at 340 nm, respectively (corresponding to 4.30 and 3.65 eV) [14–18]. The luminescence registrated by our setup originates mainly from the 340 nm band. The output signals of the photomultiplier were amplified and also formed by a CFD and then given to the TDC as stop pulses. By recording the time interval distribution in a personal computer via a direct memory interface (DMI, from IPN), the time profile of the photon emission was obtained. The profiles are non-exponential decay curves (centroids: 9 ns with POPOP and 7 ns with CsI compared to 30 ns with Coronene) measured with a

resolution of 500 ps [2]. The relative photon yields were obtained by determining the number of photons registered within the time profile per number of starting primary ions.

2.3. Sample preparation

Thin layers of POPOP or CsI were produced on an aluminized polyester foil (diameter: about 8 mm). The foil thickness was determined by optical interference to 2.1 μm. The aluminium coating had a thickness of 22 nm as established by conductivity measurements. The POPOP samples (except the 0.65 μm sample used in the ^{32}S measurements) were prepared by applying a nebulizer spray technique. Homogeneous layers of microcrystals with dimensions up to a few 100 nm were produced by this technique [2]. The thickness was determined by the amount of substance sprayed onto the foil. The CsI samples and the 0.65 μm POPOP sample were prepared by thermal evaporation. The thickness was determined by weighing using an on-line quartz-microbalance system. The surface of the CsI samples was rather plane allowing an additional precise determination of the thickness by optical interference.

3. Results

In a first experiment, the dependence of the relative photon yield Φ on the thickness of the samples has been measured. A ^{127}I beam with an initial energy of 42 MeV was chosen as suitable for this experiment. The results are depicted in Fig. 2 showing a nearly linear increase of Φ with growing sample thickness (as in [2]). In a further experiment, various primary ions of nearly the same velocity v ($v \approx 7.5 \times 10^6$ ms^{-1}) were applied to a 1 μm POPOP and to a 1.5 μm CsI sample (see Table 1). The results of the relative photon yields are depicted in Fig. 3 versus values of the electronic stopping power which were calculated by TRIM. The dashed lines in Fig. 3 represent linear fits through the data points including the origin. Obviously, the photon yield depends linearly on the electronic stopping $(dE/dx)_e$ and here also on the deposited energy ΔE when the velocity of the primary ion is kept constant, i.e. when the effective charge of the primary ion has the determining influence on the photon emission. Similar experiments with ions in different initial charge states but of the same velocity yielded the same result (not presented here).

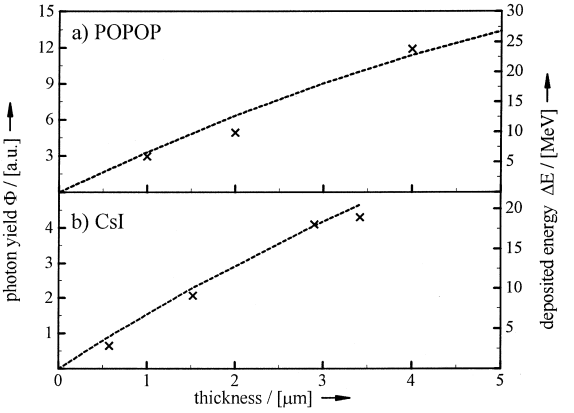

Fig. 2. The relative photon yield Φ (crosses) and the deposited energy ΔE (dashed line) at various thicknesses with POPOP (a) and with CsI samples (b) bombarded by ^{127}I at 42 MeV. The line of the ΔE values was calculated by the TRIM code and has been introduced into the figure using a suitable scaling factor.

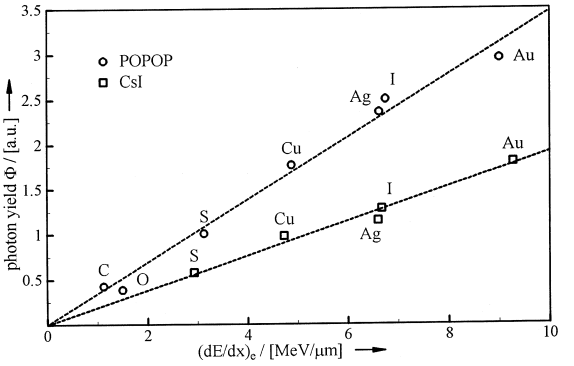

Fig. 3. Dependence of the relative photon yield Φ on the mean electronic stopping power $(dE/dx)_e$ with POPOP (circles) and with CsI (squares). The velocity of the primary ions was $v \approx 7.5 \times 10^6$ ms^{-1}. The $(dE/dx)_e$ values have been obtained from TRIM calculations. The dashed lines are linear fits. Error bars are smaller than the size of the data points.

In addition, ^{32}S ions at energies from 14 to 60 MeV were chosen as primary ions to measure the photon yield of a 0.65 μm POPOP and a 2.9 μm CsI

sample, respectively. The deposited energy has been also measured at nine different initial energies. The results are shown in Figs. 4 and 5. Both yield curves exhibit a maximum, the position of which is slightly shifted to higher energies in case of the CsI sample (Fig. 5(b)). The decrease of Φ at higher projectile energies is much more pronounced in case of the POPOP sample (Fig. 4(b)). It is interesting to note that the maxima of the yield curves do not coincide with the maxima of the deposited energy ΔE which have been determined experimentally as well as calculated with TRIM (see Figs. 4(a) and 5(a)). Both yield maxima occur at significantly higher energies than the energy loss maxima. Results obtained with a Coronene sample are very similar and show a pronounced decrease of the photon yield at higher energies as the POPOP sample (not presented here).

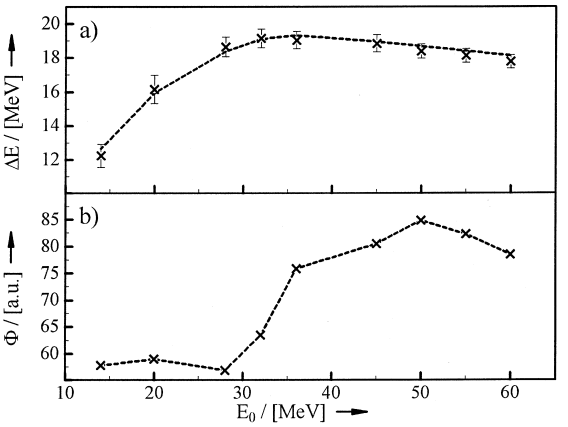

Fig. 5. Deposited energy ΔE (a) and relative photon yield Φ (b) versus initial energy E_0 of the impinging ^{32}S ion. The sample was a 2.9 μm CsI layer deposited onto an aluminized polyester foil. The ΔE has been measured (crosses) and calculated by the TRIM code (dashed line). The dashed line in (b) is drawn into the figure to guide the eye. Error bars in (b) are smaller than the data points.

4. Discussion

The nearly linear increase of the photon yield with the sample thickness observed with the 42 MeV iodine beam (see Fig. 2) indicates that the photons are produced throughout the whole sample along the ion trajectories. An almost linear increase with growing thickness occurs also for the total energy ΔE deposited in the sample (dashed curves in Fig. 2). This means that the photon production is clearly proportional to the energy deposited by the heavy ion.

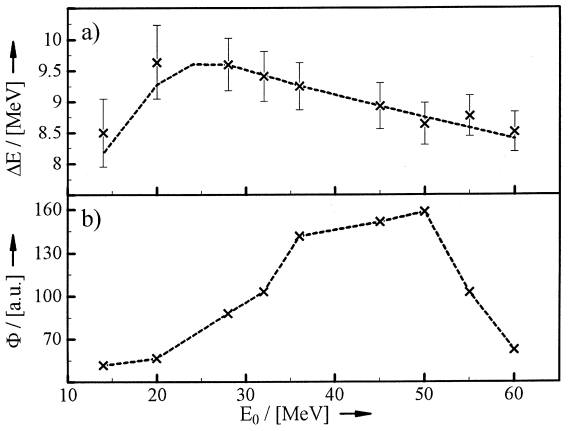

Fig. 4. Deposited energy ΔE (a) and relative photon yield Φ (b) versus initial energy E_0 of the impinging ^{32}S ion. The sample was a 0.65 μm POPOP layer deposited onto an aluminized polyester foil. The ΔE has been measured (crosses) and calculated by the TRIM code (dashed line). The dashed line in (b) is drawn into the figure to guide the eye. Error bars in (b) are smaller than the data points.

The yield curves obtained for one sample thickness with different heavy ions having all the same velocity v (see Fig. 3) exhibit the same nearly linear dependence of Φ on the deposited energy ΔE. This is equivalent with a linear dependence on the energy density. In order to make this clear we note that a large portion of ΔE goes into kinetic energy of the secondary electrons produced during the ion-matter interaction and that the range of these electrons within the sample is proportional to the square of the ion velocity. Assuming that all electrons evade perpendicular from the ion track, one obtains a cylindrical volume around this path with a radius which is given by the range of the fastest electrons. This range is identical if ions of the same velocity are chosen. Therefore the energy density increases linearly with $(dE/dx)_e$ in the present case.

The fact that the photon yields are not proportional to the deposited energy as observed for

^{32}S primary ions at different energies (see Figs. 4 and 5) demonstrates clearly that ΔE is not the relevant parameter for determining the photon yield Φ. Instead we will show that Φ is determined by the energy density existing along the ion path. For this purpose, we present calculations based on the ideas of the model of [10]. The energy density per unit path length of an incident ion $\epsilon(r)$ is given as a function of the radial distance r from the ion's track, [1]

$$\epsilon(r) = \mathcal{N}\frac{e^4}{nm_e}\frac{z^{*2}}{v^2}\frac{1}{r^2}\left[1-\frac{r}{R_{max}}\right]^{d+1/n} \quad \left[\frac{erg}{cm^3}\right] \qquad (1)$$

with $n = \frac{5}{3}$ and $d = 0.045\ \langle Z\rangle$, where $\langle Z\rangle$ is the average atomic charge of the sample defined as

$$\langle Z\rangle = \frac{\sum n_i Z_i}{\sum n_i}.$$

Z_i are the individual atomic charges. $R_{max} \simeq a(2m_e)^n v^{2n}$ is the maximum possible range of the secondary electrons with

$$a = \frac{5.025\times 10^{-12}\langle A\rangle}{0.182\times\sigma\langle Z\rangle^{8/9}}$$

according to [19]. $\langle A\rangle$ is defined as $\langle Z\rangle$. The effective charge of the impinging ion z^* is described by

$$z^* = Z\left[\frac{1-e^{-\alpha\mu}-\frac{1}{6}\alpha\mu e^{-2\alpha\mu}}{1-e^{-\mu}-\frac{1}{6}\mu e^{-2\mu}}\right] \qquad (2)$$

according to [20] with $\alpha = Z^{-2/3}$; $\mu = v/v_B$, (Z: nominal charge, v: ion velocity, v_B: Bohr velocity). The electron number density of the sample material is $\mathcal{N} = N_A\frac{\langle Z\rangle}{\langle A\rangle}\sigma$ (N_A: Avogadro number; σ: material density). The term in square brackets occurring in Eq. (1) can be attributed to the effect of electron backscattering. For the example of ^{32}S impinging at various initial energies onto a POPOP sample, Eq. (1) is depicted in Fig. 6. The different range of the secondary electrons depending on the velocity v of the incident ion is clearly demonstrated in this figure. The unit eV/V_{POPOP} (V_{POPOP}: volume of the POPOP molecule estimated to 460 Å^3) was chosen for the scale of $\epsilon(r)$ in order to use concrete molecular quantities.

[1] Units: cgs.

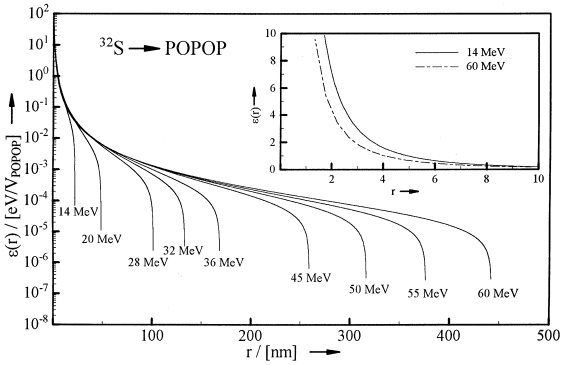

Fig. 6. Energy density $\epsilon(r)$ as a function of the radial distance r from the ion track according to Eq. (1). The curves are plotted for ^{32}S impinging at various initial energies onto a POPOP sample. In the insert $\epsilon(r)$ is shown for small r values and with two initial energies at a linear scale.

The relative photon yield is obtained in [10] as

$$\Phi_{calc} \propto \pi r_q^2\epsilon_q + \int_{r_q}^{R_{max}} 2\pi r\epsilon(r)\,dr, \qquad (3)$$

where the first term is related to the quenching mentioned above which occurs within a cylindrical volume along the ion path with radius r_q as a result of the high energy density. Eq. (3) reproduces the observed increase of Φ with increasing ion energy but it fails in describing the decrease at higher energies. Thus, we used the following approach for the calculation of the relative photon yield

$$\Phi_{calc} = \int_{r_q}^{R_{max}} 2\pi r\epsilon(r)\,dr, \qquad (4)$$

where r_q is defined by $\epsilon(r_q) = 10$ eV/V$_{POPOP}$. This approach assumes that no light is produced in an inner cylinder with radius r_q along the ion trajectory where a high energy density exists ($\epsilon(r) > 10$ eV/V$_{POPOP}$). Instead, photon emission originates only from the outer region reaching to the maximum radius R_{max} with relatively low energy densities.

That no luminescence is produced in the region of high energy density with its high degree of molecular destruction seems to be reasonable because a molecular or crystal structure, which remains intact after excitation, is a necessary

prerequisite for the generation of fluorescence in POPOP molecules or for the decay of self-trapped excitons in CsI crystals. An indication for this is the fact that the excitation happens within femtoseconds but the deexcitation processes occur in the range of nanoseconds. The value of 10 eV/V_{POPOP} has been chosen as free numerical parameter but it belongs still to a highly excited region regarding the stability of molecules. In addition, the molecular fluorescence quantum yield decreases drastically for high excitation intensities due to singlet–singlet or exciton–exciton annihilation [21,22]. In poly(p-phenylenevinylene) films for instance, the fluorescence intensity decreases clearly at excitation intensities higher than 10^{20} photons/cm^{2}s [23], leading to an energy density which is lower by several orders of magnitude than the $\epsilon(r_q)$ chosen above. Thus, the described approach appears to be rather plausible for a first approximation. It should be also noted that a similar approach is used for describing the desorption of intact molecules from samples bombarded with MeV heavy ions [24,25]. All molecules within a hot core around the ion path are assumed to break apart and intact molecules can be desorbed only from the outer region with lower energy density.

The relative photon yield as calculated according to Eq. (4) for the case that ^{32}S ions at different initial energies hit a 0.65 μm POPOP sample is given in Fig. 7. The calculated curve shows a distinct maximum at $v \approx 16.5 \times 10^6$ m/s which corresponds to an initial ^{32}S energy of 45 MeV, when v is considered as average ion velocity $\langle v \rangle$ within the sample. This is roughly in accord with the experimental data (see Fig. 4). Moreover, the calculated curve exhibits a noticeable decrease at higher velocities. This decrease is, however, less pronounced than observed for the POPOP data. The result that different experimental curves were obtained with POPOP and with CsI samples may be due to the different electronic systems of the samples which influences the luminescence probably through different quenching. Eq. (4) has been also used in order to calculate the relative photon yield which has been observed with different heavy ions of the same velocity using a POPOP sample. The result is plotted in Fig. 8 as a function of the effective heavy ion charge. The dashed curve resembles almost a quadratic function which is to be expected since Φ_{calc} is dominated by the behaviour of z^* in case of $v = \text{const}$. The agreement of Φ_{calc} with the measured data is rather satisfactory. Therefore, our approach that (i) no luminescence is produced in the region of high energy deposition and (ii) the luminescence is produced only in the region of low energy deposition has been confirmed by comparing the calculated values with our experimental results. Better quantitative agreement of calculated with measured curves can be obtained with $\epsilon(r)$ functions which describe the region of low energy deposition more precisely and which do not contain a singularity at $r = 0$.

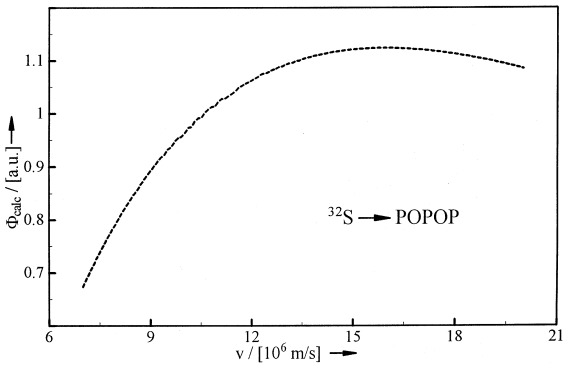

Fig. 7. Calculated photon yield Φ_{calc} versus velocity v for ^{32}S ions bombarding a 0.65 μm POPOP sample.

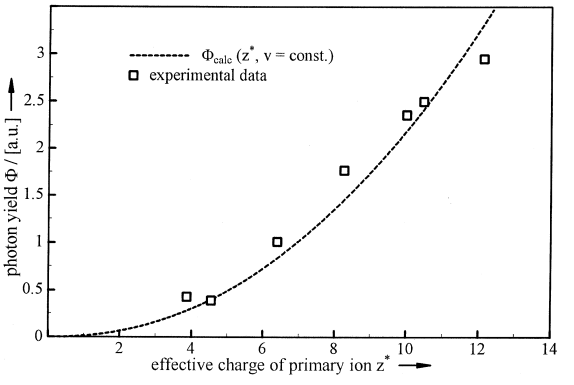

Fig. 8. Relative photon yield versus effective charge z^* of the primary ion; Φ_{calc} was calculated according to Eq. (4); the experimental data were taken from the POPOP measurements.

5. Conclusion

The luminescence induced by the bombardment of thin molecular samples with single MeV atomic ions has been measured by time-correlated single photon counting. The MeV-energy ions ($Z = 6...79$) were produced at the Erlangen tandem accelerator. The samples were layers of POPOP or CsI deposited on a thin polyester foil at a thickness which allows the ions to traverse the samples. The relative photon yield has been found to be proportional to the energy density along the ion trajectory when the initial velocity is kept constant. When the initial velocity of the primary ion was varied, a distinct maximum of the photon yield has been found which is clearly shifted to higher energies compared to the energy of the Bragg maximum. By means of calculations based on the energy deposition of the secondary electrons it was found that the observed luminescence is only produced in the region of low energy density at larger radial distances from the ion track.

Acknowledgements

The support and technical assistance of Dirk Otteken is gratefully acknowledged. This work was supported by a grant from the Deutsche Forschungsgemeinschaft (Tu 70/3-1).

References

[1] W. Tuszynski, K. Koch, E.R. Hilf, Nucl. Instr. and Meth. B 107 (1996) 160.
[2] M. Wehofsky, D. Martin, K. Koch, W. Tuszynski, E.R. Hilf, Nucl. Instr. and Meth. B 125 (1997) 71.
[3] R.G. Kaercher, E.F. da Silveira, J.F. Blankenship, E.A. Schweikert, Phys. Rev. B 51 (1995) 7373.
[4] T.R. Ariyaratne, D.D.N.B. Daya, P. Håkansson, B.U.R. Sundqvist, Int. J. Mass Spectrom. Ion Proc. 152 (1996) 31.
[5] R. Katz, E.J. Kobetich, Phys. Rev. 170 (1967) 397.
[6] M. Buenerd, D.L. Hendrie, U. Jahnke, J. Mahoney, A. Menchaca-Rocha, C. Olmer, D.K. Scott, Nucl. Instr. and Meth. 136 (1976) 173.
[7] N. Colonna, G.J. Wozniak, A. Veeck, W. Skulski, G.W. Goth, L. Manduci, P.M. Milazzo, P.F. Mastinu, Nucl. Instr. and Meth. A 321 (1992) 529.
[8] L. Muga, G. Griffith, Phys. Rev. B 9 (1974) 3639.
[9] L. Muga, M. Diksic, Nucl. Instr. and Meth. 122 (1974) 553.
[10] K. Michaelian, A. Menchaca-Rocha, Phys. Rev. B 49 (1994) 15550.
[11] J.P. Biersack, L.G. Haggmark, Nucl. Instr. and Meth. 174 (1980) 257.
[12] J.F. Ziegler, J.M. Manoyan, Nucl. Instr. and Meth. B 35 (1988) 215.
[13] V.E. Puchin, A.L. Shluger, K. Tanimura, N. Itoh, Rev. B 47 (1993) 6226.
[14] H. Lamatsch, J. Rossel, E. Saurer, Phys. Status Solidi 41 (1970) 605.
[15] H. Lamatsch, J. Rossel, E. Saurer, Phys. Status Solidi B 48 (1971) 311.
[16] W.B. Fowler, M.J. Marrone, M.N. Kabler, Phys. Rev. B 8 (1973) 5909.
[17] L. Falco, J.P. von der Weid, M.A. Aegerter, T. Iida, Y. Nakaoka, J. Phys C 13 (1980) 993.
[18] J.P. Pellaux, T. Iida, J.P. von der Weid, M.A. Aegerter, J. Phys C 13 (1980) 1009.
[19] K. Kanaya, S. Okayama, J. Phys. D 5 (1972) 43.
[20] E.C., Montenegro, S.A., Cruz, C., Vargas-Aburto, Phys. Lett. 92A, (1982), 195.
[21] H. Stiel, S. Daehne, K. Teuchner, J. Luminescence 39 (1988) 351.
[22] S. Oberländer, D. Leupold, J. Luminescence 59 (1994) 125.
[23] R.G. Kepler, V.S. Valencia, S.J. Jacobs, J.J. McNamara, Synth. Met. 78 (1996) 227.
[24] E. Nieschler, B. Nees, H. Voit, P. Beining, J. Scheer, Phys. Rev. B 37 (1988) 91.
[25] B. Sundqvist, A. Hedin, P. Håkansson, M. Salehpour, G. Säve, R. Johnson, Nucl. Instr. and Meth. B 14 (1986) 429.